Characterization of Adsorption of Sodium Dodecyl Sulfate on Charge-Regulated Substrates by Atomic Force Microscopy Force Measurements

Kai Hu and Allen J. Bard*

Department of Chemistry and Biochemistry, The University of Texas at Austin, Austin, Texas 78712

Received May 9, 1997[⊗]

The adsorption of sodium dodecyl sulfate (SDS) on gold surfaces covered with self-assembled monolayers (SAMs) of thiols made with either hexadecyl mercaptan or 2-aminoethanethiol hydrochloride was investigated by probing the surface charge. This was accomplished by determining the force between a modified (with a negatively charged silica sphere) tip of an atomic force microscope and the surface as SDS was adsorbed. The ionic nature of aqueous SDS solutions and the critical micelle concentration (cmc) in deionized water were determined by measuring the sudden change in diffuse double-layer thickness on micelle formation. The interaction between a silica probe and an initially positively charged gold substrate with a 2-aminoethanethiol layer was a strong function of SDS concentration. The phenomenon of surface charge reversal (where the amount of negative SDS equals the cationic surface charge) was directly observed at an SDS concentration of about 1/1000 cmc. The surface electrostatic potentials of the surfactant-adsorbed substrates were calculated by solving the complete nonlinear Poisson−Boltzmann equation with the knowledge of silica probe surface potentials. From the surface charge vs surfactant concentration data, the adsorption behavior of SDS was assessed. The interaction between the silica probe and the hydrophobic hexadecyl mercaptan SAM-covered gold substrate was also examined to mimic the adsorption behavior of the hydrophobic hemimicelle, which could form on the 2-aminoethanethiol surface. Considerably different surfactant adsorption behavior was found for the hydrophobic hexadecyl mercaptan SAM and the 2-aminoethanethiol surfaces. For the adsorption of SDS on an initially positively charged surface, quantitative force measurements show that the formation of a compact and uniform hemimicelle or bilayer did not occur.

Introduction

Adsorption of surfactants on solid surfaces is a phenomenon of great importance to many industrial processes such as colloidal stabilization, ore flotation, detergency, and petroleum recovery. Although the process of surfactant aggregation and micelle formation and the structures of these aggregates are well understood in free solutions,[1] it is not clear how these surfactant aggregates or micelles are affected by the presence of a solid surface. For many years, the adsorption properties of surfactants on solid surfaces have been the subject of intensive studies, with regard both to the amount of adsorption and to the structure of the adsorbed layer. Generally, interfacial adsorption isotherms have been used for describing the adsorption characteristics of surfactants at the solid/liquid interface. Several experimental techniques such as NMR,[2] ellipsometry,[3] FTIR,[4] Raman,[5] and ESR[6] have been employed to elucidate adsorption mechanisms. More recently, fluorescence decay[7] and neutron reflection[8] have been used. From such studies, some aspects of surfactant adsorption to solid surfaces are clear. For example, charged surfactants adsorb readily by electrostatic interactions on oppositely charged surfaces. A characteristic feature of surfactant adsorption at concentrations below the critical micelle concentration (cmc) is that adsorbed surfactants form local aggregates on the surface.

The structure of surface aggregates and the adsorption mechanisms continue to be subjects of investigation. Different models have been proposed to describe the adsorption of ionic surfactants on oppositely charged surfaces. The reverse orientation model proposed by Somasundaran and Fuerstenau[9] has been particularly successful for describing anionic surfactant adsorption on alumina[9] and rutile.[10,11] In the four-region model, four distinct adsorption regions are suggested from the log−log scale adsorption isotherms for these systems. According to this model, in very dilute surfactant solutions, the surfactants adsorb electrostatically as individual ions (monomers) in region 1 and associate into hemimicelles (local zones of compact organized surfactants) in region 2 with an increase in surfactant concentration. In the hemimicelle, the surfactants are oriented with their charged head groups toward the solid surface, while the hydrocarbon chains protrude into the solution, thus forming a hydrophobic surfactant monolayer on the surface. Further increases in surfactant concentration lead to region 3 where local bilayer structures build up on the sites already formed in region 2 with a characteristic surface charge reversal. Finally, at solution concentrations near the cmc, a plateau region (region 4) is observed, where the adsorbed layer possesses the structure of a bilayer. Harwell et al.[12,13] later presented a surface bilayer model which is slightly different from the reverse orientation model. In this model, following the initial individual

⊗ Abstract published in *Advance ACS Abstracts*, September 1, 1997.

(1) Rosen, M. J. *Surfactants and Interfacial Phenomena*; Wiley: New York, 1989.
(2) Soderlind, E.; Stilbs, P. *J. Colloid Interface Sci.* **1991**, *143*, 586.
(3) Wangnerud, P.; Olofsson, G. *J. Colloid Interface Sci.* **1992**, *153*, 392.
(4) Montgomery, M. E., Jr.; Wirth, M. J. *Anal. Chem.* **1992**, *64*, 2566.
(5) Somasundaran, P.; Kunjappu, J. T.; Kumar, C. V.; Turro, N. J.; Barton, J. K. *Langmuir* **1989**, *5*, 215.
(6) Esumi, K.; Sugimura, A.; Yamada, T.; Meguro, K. *Colloids Surf.* **1992**, *62*, 249.
(7) Chandar, P.; Somasundaran, P.; Turro, N. J. *J. Colloid Interface Sci.* **1987**, *117*, 31.
(8) McDermott, D. C.; McCarney, J.; Thomas, R. K.; Rennie, A. R. *J. Colloid Interface Sci.* **1994**, *162*, 304.
(9) Somasundaran, P.; Fuerstenau, D. W. *J. Phys. Chem.* **1966**, *70*, 90.
(10) Böhmer, M. R.; Koopal, L. K. *Langmuir* **1992**, *8*, 2649.
(11) Böhmer, M. R.; Koopal, L. K. *Langmuir* **1992**, *8*, 2660.
(12) Harwell, J. H.; Hoskins, J. C.; Schechter, R. S.; Wade, W. H. *Langmuir* **1985**, *1*, 251.
(13) Yeskie, M. A.; Harwell, J. H. *J. Phys. Chem.* **1988**, *92*, 2346.

S0743-7463(97)00483-6 CCC: $14.00

surfactant ion adsorption, local bilayer structures begin to form on patches of the solid surface at a critical solution concentration without the intermediate formation of a hemimicelle. These patches of surfactant bilayers were proposed to form in region 2 of the reverse orientation model. More recently, Gu and co-workers[14] proposed a two-step adsorption model based on a linear scale adsorption isotherm. In the first step, the monomer adsorption is driven by electrostatic attraction between the ionic surfactant head group and the oppositely charged surface. Complete monolayer coverage results in the first-stage plateau. In a second step, with an increase in surfactant concentration, small surface micelles form around the initial adsorption sites by lateral hydrophobic interactions, effecting charge reversal of the adsorbed surface. Complete surface coverage leads to the second-stage plateau near the cmc. Clearly, all these models assume the same driving forces for ionic surfactant adsorption: the electrostatic attractive forces between the surface and the ionic surfactant head group and the lateral hydrophobic attraction between the hydrocarbon chains. Although considerable advances have been made in our understanding of the surfactant adsorption at the solid/liquid interface, a number of issues are still not well understood. For example, does the formation of the bilayered aggregates proceed directly from adsorbed monomers or via hemimicelles; i.e., does the modifying layer grow by a layer-by-layer mechanism or do local thicker structures nucleate and form before a monolayer is completed? Over what surfactant concentration range does the surface charge reversal take place? Is the hemimicelle really a compact hydrophobic monolayer as proposed? Do the surfactants form a uniform and flat bilayer near the cmc? In this paper, we address some of these questions. We investigate the adsorption of an ionic surfactant on charge-regulated surfaces by measuring the interfacial forces between a charged tip of an atomic force microscope (AFM) and the surface at different stages of surfactant layer formation. More precisely, the diffuse double layer at the surface with absorbed surfactant is probed at nanometer separation and with nanonewton force resolution with a modified tip on the cantilever of an AFM. The surface charge and potential are then calculated from the force data.

The direct measurement of surface forces has received considerable attention and has provided significant insight into the understanding of interfacial processes.[15] These force measurements have been achieved primarily with two instruments, the surface forces apparatus (SFA)[16] and the AFM.[17] The SFA has been applied mainly to the measurement of forces between mica surfaces and materials adsorbed on mica.[18] The AFM, initially used in a purely imaging capacity, has recently been employed to measure surface forces.[19] The most quantitative of these AFM force measurements has involved the attachment of a spherical tip to a microfabricated cantilever to provide a larger tip area and a well-defined tip geometry, thus allowing direct comparison to theory. One of the advantages of AFM force measurement over that of the SFA is the virtually unlimited choice of substrates. The SFA has been used mainly to measure the surface forces between two mica surfaces, e.g., with adsorbed cetyltrimethylammonium bromide (CTAB), a cationic surfactant.[20,21] Very recently, AFM force measurements have also been conducted between two CTAB adsorbed silica surfaces at a surfactant concentration above the cmc.[22] The SFA studies generally confirmed the formation of a hydrophobic monolayer of CTA^+ ions on mica at CTAB concentrations below the cmc and a highly charged hydrophilic bilayer near the cmc. All of these studies were limited to a cationic surfactant (a choice of a negatively charged substrate). Moreover, the force measurements in all these investigations were conducted between two surfaces of the same material. The adsorption of surfactants on both surfaces might complicate the data interpretation, i.e., in determining explicitly the sign of the surface charge from a repulsive force curve.

In the present work, we systematically investigated the adsorption properties of an anionic surfactant, sodium dodecyl sulfate (SDS), on charge-regulated surfaces using the AFM force measurements over a broad range of SDS concentrations. Self-assembled monolayers (SAMs), prepared by the spontaneous chemisorption of thiolates on gold, were used to create positively charged or hydrophobic surfaces by choosing suitable terminal functional groups. Under the given conditions, the modified silica probe surface was negatively charged, so SDS adsorption only occurred at the substrate, thus offering a better opportunity to study the adsorption process on the substrate. The force-measuring experiment is illustrated in Chart 1. From a series of force measurements at different SDS concentrations, the phenomenon of surface charge reversal was directly observed at a surprisingly low SDS concentration. By correlating the surface charge to SDS concentration, information about the surfactant adsorption mechanism was obtained. To our knowledge, this is the first demonstration of using an AFM to observe directly surface charge reversal through surfactant adsorption.

Experimental Section

Reagents. 2-Aminoethanethiol hydrochloride, hexadecyl mercaptan, and SDS (99%) were from Aldrich and were used as received. Solutions of NaCl and SDS were freshly prepared with 18 MΩ deionized water (Milli-Q Plus, Millipore Corp., Bedford, MA). The solution pH values were adjusted with 0.01 M HCl and 0.01 M NaOH. Immediately before use, the solutions were deaerated with argon for 20 min.

Probe and Substrate Preparation. Silica probe preparation has been described before.[19b,23,24] In brief, under an optical microscope (Olympus, Model BHTU, Tokyo, Japan), a 10−20 μm silica sphere (Polysciences, Warrington, PA) was glued near the apex of a commercial, standard V-shaped, silicon nitride cantilever (Nanoprobe, Park Scientific, Mountain View, CA) with a low melting point epoxy resin (Epon 1002, Shell, Houston, TX).

(14) (a) Gu, T.; Huang, Z. *Colloids Surf.* **1989**, *40*, 71. (b) Gao, Y.; Du, J.; Gu, T. *J. Chem. Soc., Faraday Trans. 1* **1987**, *83*, 2671.

(15) (a) Derjaguin, B. V.; Rabinovich, Y. I.; Churaev, N. V. *Nature* **1978**, *272*, 313. (b) Israelachvili, J. N. *Intermolecular and Surface Forces*, 2nd ed.; Academic Press: New York, 1991.

(16) (a) Israelachvili, J. N.; Adams, G. E. *J. Chem. Soc., Faraday Trans.* **1978**, *74*, 975. (b) Horn, R. G.; Israelachvili, J. N. *J. Chem. Phys.* **1981**, *75*, 1400. (c) Parker, J. L.; Christenson, H. K.; Ninham, B. W. *Rev. Sci. Instrum.* **1989**, *60*, 3135.

(17) Binnig, G.; Quate, C.; Gerber, G. *Phys. Rev. Lett.* **1986**, 56, 930.

(18) (a) Crassous, J.; Elisabeth, C.; Gayvallet, H.; Loubet, J. L. *Langmuir* **1993**, *9*, 1995. (b) Shubin, V.; Kekicheff, P. *J. Colloid Interface Sci.* **1993**, *155*, 108. (c) Marra, J.; Hair, M. L. *J. Phys. Chem.* **1988**, *92*, 6044. (d) Parker, J. L.; Christenson, H. K. *J. Chem. Phys.* **1988**, *88*, 8013.

(19) (a) Ducker, W. A.; Senden, T. J.; Pashley, R. M. *Nature* **1991**, *353*, 239. (b) Ducker, W. A.; Senden, T. J.; Pashley, R. M. *Langmuir* **1992**, *8*, 1831. (c) Biggs, S.; Mulvaney, P.; Zukoski, C. F.; Grieser, F. *J. Am. Chem. Soc.* **1994**, *116*, 9150. (d) Larson, I.; Drummond, C. J.; Chan, D. Y. C.; Grieser, F. *J. Am. Chem. Soc.* **1993**, *115*, 11885. (e) Li, Y. Q.; Tao, N. J.; Pan, J.; Garcia, A. A.; Lindsay, S. M. *Langmuir* **1993**, *9*, 637. (f) Atkins, D. T.; Pashley, R. M. *Langmuir* **1993**, *9*, 2232. (g) Larson, I.; Drummond, C. J.; Chan, D. Y. C.; Grieser, F. *J. Phys. Chem.* **1995**, *99*, 2114.

(20) Kekicheff, P.; Christenson, H. K.; Ninham, B. W. *Colloids Surf.* **1989**, *40*, 31.

(21) (a) Pashley, R. M.; McGuiggan, P. M.; Horn, R. G.; Ninham, B. W. *J. Colloid Interface Sci.* **1988**, *126*, 569. (b) Pashley, R. M.; Israelachvili, J. N. *Colloids Surf.* **1981**, *2*, 169.

(22) Johnson, S. B.; Drummond, C. J.; Scales, P. J.; Nishimura, S. *Langmuir* **1995**, *11*, 2367.

(23) Hillier, A. C.; Kim, S.; Bard, A. J. *J. Phys. Chem.* **1996**, *100*, 18808.

(24) Hu, K.; Bard, A. J. *Langmuir* **1997**, *13*, 5114.

Chart 1. Schematic Representation of the AFM Force Measurement between a Negatively Charged Silica Sphere and a Positively Charged SAM-Covered Gold Substrate in an SDS Solution Where Surface Charge Reversal Has Already Taken Place

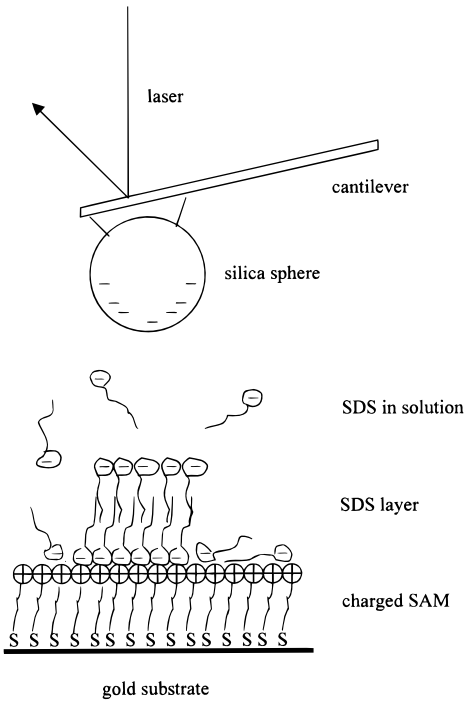

Care was exercised to avoid coating the molten resin on the reflective gold side of the cantilever. Immediately before use, the silica probe was cleaned by rinsing with EtOH, followed by copious amounts of purified water, and drying with argon.

Silica substrates were prepared from commercial glass cover slips (M6045-2, Baxter Healthcare Corp., McGaw Park, IL). Before each experiment, the silica substrates were cleaned in a concentrated nitric/sulfuric acid (1:1) solution and rinsed thoroughly with deionized water followed by exposure to condensing steam vapor for 30 min. AFM images obtained from the silica surfaces indicated a mean roughness of 1.1−1.4 nm/μm^2 with a maximum peak to valley height of 3.5−4.7 nm over a 1 μm square.

Large, flat, template-stripped gold surfaces were prepared by the method of Hegner et al.[24,25] Briefly, gold was vacuum deposited onto freshly cleaved mica sheets. The vapor-deposited gold surface (200 nm thick) was glued (Epo-tek No. 377, Polyscience) to a piece of precleaned Si wafer. After chemical stripping (in THF) of the gold from the mica, a smooth gold surface on Si was obtained. AFM images of this type of template-stripped gold surface showed a mean roughness of 0.20−0.33 nm/μm^2 with a maximum peak to valley height of 2.5−2.8 nm over a 1 μm square. The freshly prepared template-stripped gold surface was immediately immersed in a 5 mM 2-aminoethanethiol hydrochloride or 5 mM hexadecyl mercaptan ethanolic solution for over 24 h. Prior to use, the SAM-covered gold substrate was rinsed with EtOH for 30 s and dried under argon.

Force Measurements. All force−distance data were obtained from a Nanoscope III AFM (Digital Instruments, Santa Barbara, CA) equipped with a piezo scanner having a maximum scan range of 15 μm × 15 μm × 2 μm. The piezo scanner calibration was achieved as described earlier.[23,24] The AFM was operated in the force mode, in which the *xy* raster motion of the sample on the piezoelectric crystal is suspended and the substrate is moved toward and away from the cantilever in the *z* direction by applying a sawtooth voltage. Therefore, the force between a surface and the AFM tip is measured as a function of the separation between the surface and tip. In a typical experiment, the silica probe was mounted into a precleaned AFM liquid cell (Digital Instruments). The solution with an accurately controlled salt concentration and pH was injected into the liquid cell. After about 20 min of equilibration time, the force−distance data were collected from different locations of the substrate.

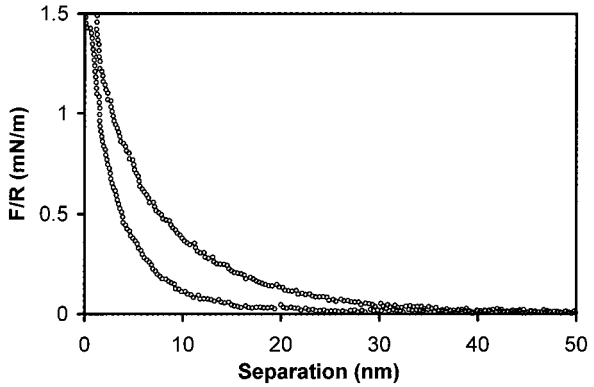

Figure 1. Force between a silica probe and a silica substrate in 10^{-2} M NaCl (lower curve) and 10^{-2} M SDS (upper curve) aqueous solutions at pH 9.0. The force is scaled to the probe radius (R = 8.0 μm).

AFM Data Analysis. During the acquisition of a force curve, cantilever deflections are monitored by recording the changes in voltage in a split photodiode, onto which is focused a laser beam that is reflected from the backside of the cantilever. The substrate *z* direction displacement is given by the piezo scanner voltages. The raw data giving the tip deflection vs substrate displacement are converted to a normalized force (force/radius, F/R) vs tip−substrate separation, d, with knowledge of the cantilever spring constant, k, and tip radius, R. This conversion requires knowing the zero force position, defined as the photodiode signal at large separations, where a change in the substrate position (piezo *z* direction displacement) has no effect on cantilever deflection. Zero separation is defined as the point where a change in substrate position causes an equal change in the cantilever deflection, the so-called constant compliance region.

As in earlier studies,[23,24] k was determined using the method of Cleveland et al.[26] and was found to be 0.65 ± 0.12 N/m (cf. the manufacturer's nominal value of 0.58 N/m). Derjaguin−Landau−Verwey−Overbeek (DLVO) theory[27] was employed to calculate the surface electrostatic potentials between the similarly charged surfaces. The electrical double-layer interaction energy between dissimilarly charged surfaces was calculated for the constant-potential or constant-charge limits of the complete nonlinear Poisson−Boltzmann equation using the method of Hillier et al.[23] The Hamaker constants (A_H) for the silica−silica and silica−gold interactions were 0.88 × 10^{-20} J[28] and 1.1 × 10^{-19} J,[24] respectively.

Results and Discussion

Ionic Nature of SDS in Aqueous Solutions. Knowledge of the ionic nature of SDS in aqueous solutions is important for understanding the SDS adsorption processes on charge-regulated substrates discussed later. Information about the ionic nature of SDS solutions can be obtained by comparing double-layer (dl) forces between a silica probe and a silica substrate in NaCl and SDS solutions of different concentrations. The silica surfaces are negatively charged at pH 9.0, and diffuse double layers form at the interfaces. AFM force (F/R vs d) measurements can probe the dl structure and thickness as the tip penetrates the dl. Figure 1 compares the silica−silica interaction force

(25) Hegner, M.; Wagner, P.; Semenza, G. *Surf. Sci.* **1993**, *291*, 39.

(26) (a) Cleveland, J. P.; Manne, S.; Bocek, D.; Hansma, P. K. *Rev. Sci. Instrum.* **1993**, *64*, 403. (b) Sader, J. E.; Larson, I.; Mulvaney, P.; White, L. R. *Rev. Sci. Instrum.* **1995**, *66*, 3789.

(27) (a) Derjaguin, B. V. *Trans. Faraday Soc.* **1940**, *36*, 203. (b) Derjaguin, B. V.; Landau, L. D. *Acta Phys. Chem.* **1941**, *14*, 633. (c) Derjaguin, B. V.; Landau, L. D. *J. Exp. Theor. Phys.* **1941**, *11*, 802. (d) Verwey, E. J. W.; Overbeek, J. T. G. *Theory of the Stability of Lyophobic Colloids*; Elsevier: New York, 1948.

(28) (a) Grabbe, A.; Horn, R. G. *J. Colloid Interface Sci.* **1993**, *157*, 375. (b) Hunter, R. J. *Foundations of Colloid Science*; Oxford University Press: Oxford, 1987. (c) Hough, D. B.; White, L. R. *Adv. Colloid Interface Sci.* **1980**, *81*, 285.

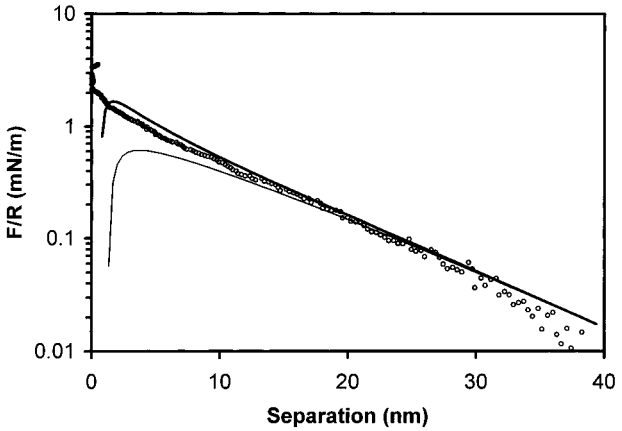

Figure 2. Measured (circles) and theoretical (solid lines) force between a silica probe and a silica substrate at constant charge (thick line) and constant potential (thin line) in a 7×10^{-3} M SDS aqueous solution at pH 9.0. The Debye length was obtained by fit of the force curve to DLVO theory with $A_H = 0.88 \times 10^{-20}$ J. The best fit parameters for all force curves are given in Table 1.

Table 1. Force Data Analysis Results of Silica−Silica Interactions in SDS Aqueous Solutions[a]

SDS conc (mM)	1.0	3.0	5.0	6.0	7.0	8.0	10.0
Debye length, κ^{-1} (nm)	9.63	5.57	4.55	4.32	9.63	8.81	7.88
free Na^+ concn (mM)	1.0	3.0	4.5	5.0	1.0	1.2	1.5
% of free Na^+	100.0	100.0	90.0	83.3	14.3	15.0	15.0

[a] Force data were obtained between a silica sphere and a silica substrate in aqueous solutions of different SDS concentrations at 25 °C and pH 9.0. The Debye length was obtained by fit of the force curve to DLVO theory. All these calculations include both electrostatic and van der Waals interactions with $A_H = 0.88 \times 10^{-20}$ J. Free Na^+ ion concentration was calculated from eq 1.

curves in 10^{-2} M NaCl and 10^{-2} M SDS aqueous solutions at pH 9.0, with the force scaled to the probe radius. Note that the dl force in 10^{-2} M SDS solution extends further into the solution than in 10^{-2} M NaCl solution, indicating a lower free ion concentration in the 10^{-2} M SDS solution. However, the force curves obtained in 10^{-3} M NaCl and 10^{-3} M SDS solutions were exactly the same (not shown). A series of silica−silica interaction force curves were collected in SDS solutions of concentrations ranging from 1.0 to 10.0 mM at pH 9.0. Generally, these force−distance curves exhibited an exponential dependence with distance that was well reproduced by standard DLVO theory.[27] These force data, when fit to the sum of repulsive electrostatic and attractive van der Waals interactions, with $A_H = 0.88 \times 10^{-20}$ J, provide the silica surface potential and Debye length, κ^{-1}, of the diffuse dl. For dilute aqueous solution containing 1:1 electrolyte at 25 °C, the Debye length is given by

$$\kappa^{-1} = 0.3045/C^{1/2} \quad (1)$$

where C is the free ion concentration of the electrolyte. Figure 2 shows the force curve measured between the silica probe and the silica substrate in 7 mM SDS aqueous solution at pH 9.0, with the best fit theoretical force curves at a constant surface charge (thick line) and constant surface potential (thin line) limit. The best fit parameters for all force curves are given in Table 1.

The ionic property of SDS will be different at concentrations of SDS below and above the cmc because of micelle formation. There are well-established experimental methods to determine the cmc of a surfactant.[1] Generally, these methods utilize a sudden change in a physical property

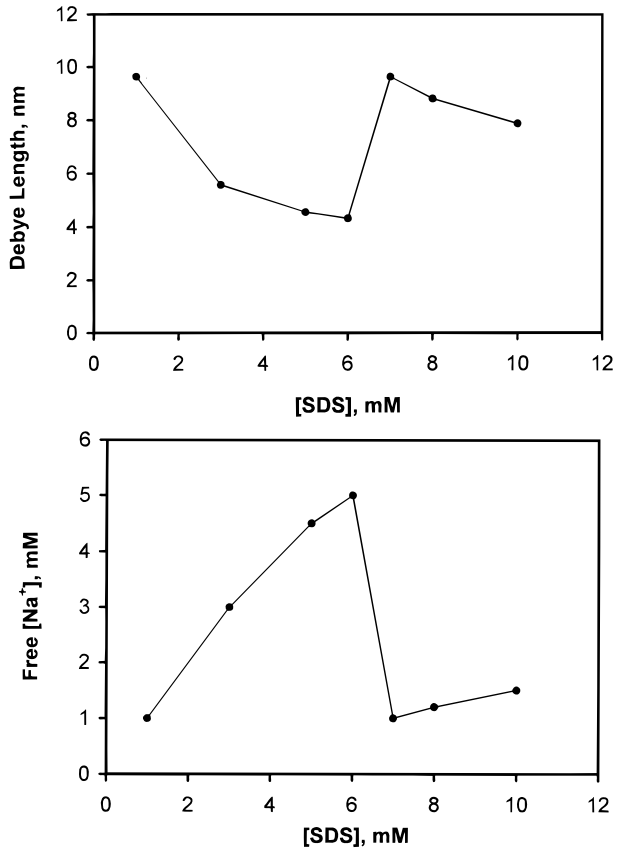

Figure 3. (a, top) Effect of SDS concentration on Debye length, κ^{-1}, of the diffuse double layer. (b, bottom) Effect of SDS concentration on solution free Na^+ ion concentration. Force data between the silica probe and the silica substrate were collected in SDS aqueous solutions of different concentrations at pH 9.0.

(surface tension, conductivity, fluorescence, light scattering, or osmotic pressure) of the solution, the surfactant, or a probe molecule. Here we measure the cmc of SDS in deionized water by noting the sudden change in the diffuse dl thickness at the cmc. When the Debye length, κ^{-1}, and the corresponding free Na^+ ion concentration are plotted against solution SDS total concentration, the results in Figure 3 are obtained. As shown, both κ^{-1} and the free Na^+ ion concentration calculated from the surface force experience a sudden change at an SDS concentration between 6 and 7 mM. Below 3 mM, the dl forces are well-described by assuming the surfactant to be a completely dissociated simple 1:1 electrolyte like NaCl. In 5 or 6 mM SDS solution, the free Na^+ ion concentration decreases 10−17%, probably because some of the Na^+ ions bind to the surfaces of premicellar aggregates in these solutions. Near 7 mM, micelles form in the solution and most of the Na^+ ions (up to 85%) bind to the micelle surfaces to compensate the highly charged micelles. The phenomenon of ion binding is well-known[1] and leads to a sudden decrease in free Na^+ ion concentration in the solution and to a sudden increase in the thickness of the diffuse dl at the silica surface. Therefore, the concentration of 7 mM represents the cmc of SDS in deionized water measured by this technique; this is slightly lower than the typical cmc of 8.1−8.4 mM reported for SDS in deionized water.[1] Above 7 mM, the ratio of Na^+ ions bound to the micelle surfaces remains constant at 85%, although the solution SDS total concentration changes. The Debye lengths observed in the micellar solutions appear to support the hypothesis that only the counterions (Na^+) contribute to the Debye length, with no apparent contribution from charged micelles and their bound counterions. The good

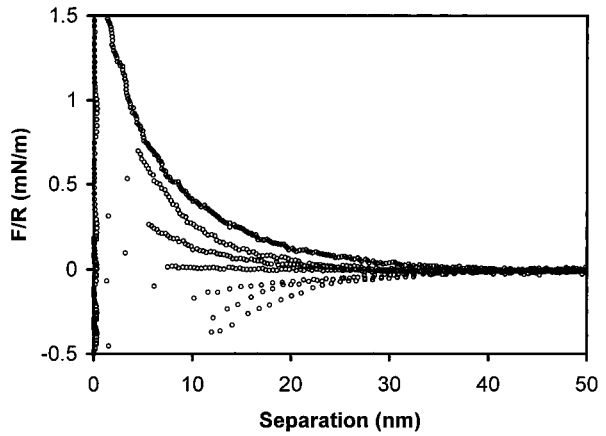

Figure 4. Force between a silica probe ($R = 8.0\ \mu$m) and positively charged gold substrate in aqueous solutions of different SDS concentrations at pH 5.0. The total salt concentration ($C_{SDS} + C_{NaCl}$) was maintained at 10^{-3} M. The force curves correspond to SDS concentrations, from bottom to top, of 0, 10^{-7}, 10^{-6}, 5×10^{-6}, 10^{-5}, 10^{-4}, and 10^{-3} M. The phenomenon of surface charge reversal is observed at an SDS concentration of about 5×10^{-6} M.

fit of the force curves to the dl theory of a 1:1 electrolyte also supports the counterion-only hypothesis, although there must be a significant density of micelles in the solution. These findings are consistent with previous results from the SFA force measurements between two mica surfaces in CTAB micellar solutions.[21a,29] Nevertheless, the theory concerning the nature and range of dl forces between two surfaces in the presence of a highly asymmetric electrolyte like a micellar solution is still not well-understood. We did not carry out additional AFM force measurements to elucidate the micelle behavior in the solution and the effect of its formation on the dl forces.

Adsorption of SDS on a Positively Charged Substrate. Force measurements between a silica probe and a silica substrate were conducted to determine the silica probe surface potential (ψ_p) under conditions similar to those found while probing the dl at surfactant adsorbed substrates. Solutions of NaCl, SDS, and a mixture of both species were examined. At solution pH 5.0, the silica surface is negatively charged, and the measured silica surface potential is −37 mV for all 1 mM solutions and −30, −35, and −34 mV for 5, 8, and 10 mM SDS solutions, respectively. There is no evidence showing that SDS adsorbs on a negatively charged silica surface under any of the conditions examined.

To obtain smooth and reproducible force curves at different locations on a substrate, a very smooth substrate surface is needed for the AFM force measurements. We choose gold as the substrate simply because a large and smooth (nanometer scale) gold surface can be prepared easily. SAMs prepared by spontaneous chemisorption of thiolates on gold were used to create positively charged surfaces. In this case, 2-aminoethanethiol hydrochloride was the SAM species. The surface pK_a for the terminal amino group was determined to be 6.9 ± 0.5 by measuring the differential interfacial capacitance.[30] Thus when solutions of pH 5.0 were used, most of the surface-confined amino groups should be protonated, thus offering a positively charged substrate.

The interaction between a silica probe and a positively charged gold substrate was a strong function of SDS concentration. In Figure 4, we show typical force−separation curves obtained in aqueous solutions of different SDS concentrations at pH 5.0. The total salt concentration ($C_{SDS} + C_{NaCl}$) was maintained at 10^{-3} M for each solution. In 10^{-3} M NaCl solution without SDS, an electrostatic attractive force was observed, demonstrating that the gold substrate was indeed positively charged. Note that the tip snaps to the substrate prior to contact at about 12 nm in this force curve. The reproducibility of the snap-in distance is generally poor in AFM force measurements. Typically, attractive forces existing at separations of less than the snap-in distance are inaccessible, a limitation of using a passive cantilever. At an SDS concentration of 10^{-8} M, the measured force curve was identical to that obtained from the solution without SDS, indicating that the adsorption-induced surface charge change was below the force detection limit of the cantilever used. From 10^{-7} to 5×10^{-6} M, the electrostatic attractive force decreased as the SDS concentration increased. This decrease in attractive force can be attributed to a decrease in positive charge of the substrate, caused by SDS adsorption driven by electrostatic attraction between SDS head groups and positively charged surface sites. Each adsorbed DS^- ion compensates a surface positive charge and thus contributes to the attenuation of the positive charge on the substrate. At an SDS concentration of 5×10^{-6} M, there were no measurable long range electrostatic interactions between silica and an SDS-adsorbed gold substrate, showing that the film-covered gold substrate was uncharged; i.e., a hydrophobic hemimicelle formed on the gold substrate, or less likely, the positive ions and negative ions were equally distributed over the substrate. Above concentrations of 5×10^{-6} M, an electrostatic repulsive force was observed, which was a clear indication of the reversal of the original surface charge. Apparently, additional surfactant ions were adsorbed by lateral hydrophobic interactions in this concentration range, effecting a charge reversal of the substrate. Given the cmc of 7−8 mM for SDS, it is quite surprising that the phenomenon of surface charge reversal occurs at such a low SDS concentration of about 1/1000 cmc, as compared to the previously reported value of about 1/20 cmc for the adsorption of CTAB on mica.[21b] In a separate experiment, when NaCl was not added to SDS solution, the surface charge reversal happened at about the same SDS concentration ($(0.5-1) \times 10^{-5}$ M), indicating that the solution ionic strength did not strongly affect the surface charge reversal process. With increases in SDS concentration, the electrostatic repulsive force increased further, signaling negative charge building up on the substrate. With SDS concentrations above 10^{-3} M (not shown in Figure 4), the repulsive force started to decrease due to the compression of the diffuse dl caused by higher salt concentration.

In Figure 4, the dl force change with SDS concentration between the negatively charged silica tip and the SDS-adsorbed gold substrate can be explained in terms of both the nature of the dl and the state of the adsorption process. In the force measurement, the silica spherical tip probes the diffuse dl near the gold substrate as it moves through the dl, which consists of counterions that compensate the charge residing at the SDS-adsorbed gold/solution interface. For example, in 10^{-3} M SDS solution, where the surface charge reversal has already taken place, the net surface charge of the gold substrate becomes negative and a diffuse dl with a net positive charge forms near the gold substrate, which consists of a higher local concentration of Na^+ (and H^+) and a lower local concentration of DS^- (and OH^-). Therefore, an electrostatic repulsive dl interaction force is obtained as the negatively charged silica probe (with its own positively charged diffuse dl) penetrates through this dl near the gold substrate.

(29) Pashley, R. M.; Ninham, B. W. *J. Phys. Chem.* **1987**, *91*, 2902.
(30) Bryant, M. A.; Crooks, R. M. *Langmuir* **1993**, *9*, 385.

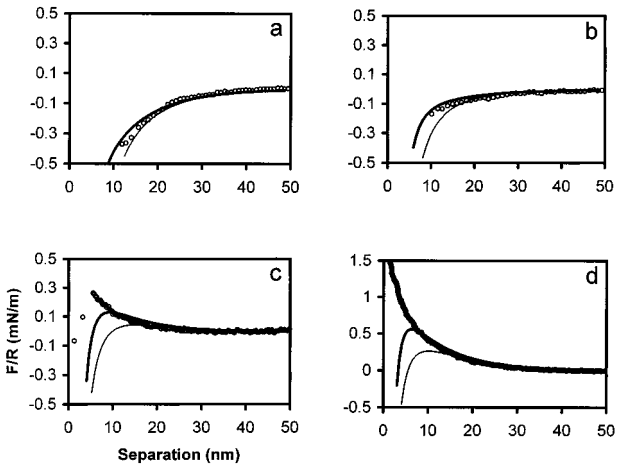

Figure 5. Measured (circles) and theoretical (solid lines) forces between a silica probe and a positively charged gold substrate at constant charge (thick line) and constant potential (thin line) in aqueous solutions (pH 5.0) of (a) 0, (b) 10^{-6}, (c) 10^{-5}, and (d) 10^{-3} M SDS. $\psi_p = -37$ mV for all 10^{-3} M solutions. The best fit parameters for all force curves are given in Table 2.

The surface electrostatic potentials (ψ_s) of the SDS-adsorbed gold substrate can be calculated from the force data. Generally, for similarly charged surfaces at low surface potentials, the linearized form of the Poisson−Boltzmann equation yields the same results as the DLVO theory. For dissimilarly charged surfaces, the complete nonlinear Poisson−Boltzmann equation must be solved due to the presence of an additional Maxwellian stress term that represents an induced image charge. In this work, the method of Hillier et al.[23] was used to calculate the electrical dl interaction. The surface electrostatic potentials of SDS-adsorbed gold substrates were obtained by theoretical fits of the force data to solutions of the complete nonlinear Poisson−Boltzmann equation with the knowledge of the silica probe surface potential. Figure 5 shows the results of theoretical curves fit to experimental force data at several selected SDS concentrations. All these calculations include both electrostatic and van der Waals interactions, with $A_H = 1.1 \times 10^{-19}$ J[24] and $\kappa^{-1} = 9.63$ nm for a solution concentration of 10^{-3} M. The upper curve (thick line) is for the model at a constant surface charge limit for both the tip and substrate, while the lower curve (thin line) is at a constant surface potential. As shown, although the constant surface charge boundary conditions more closely reflect the experimental data, neither constant surface charge conditions nor constant surface potential conditions represent a good fit to force data at separations of less than 10 nm. Several factors that are probably responsible for the deviation between theoretical curves and force data at small separations have been discussed previously.[23,24] These factors are the inaccuracy of the measured A_H value for the silica−gold interaction, an uncertainty in the location for the plane of surface charge due to the roughness of the silica probe and the gold substrate, and the exclusion of a solvent repulsion term from the theoretical curves. In this work, we emphasize the determination of the plane of surface charge. At high SDS concentrations, the adsorbed surfactants form bilayer films or small surface micelles on the substrate; this will cause the location of the plane of surface charge to shift further into the solution. Indeed, for each of these repulsive force curves, a slightly better fit was obtained with the plane of surface charge moved 3 nm (approximate thickness of the SDS bilayer) positive of the contact position. However, for lower SDS concentrations, especially before the surface charge reversal takes place, the location of the plane of surface charge is the original positive charge plane of the substrate. For comparison of the data analysis results in all of these fits, the plane of surface charge was taken as the onset of the contact region of the force measurement. In Figure 5a, the force curve obtained in 10^{-3} M NaCl without SDS at pH 5.0, the best fit gives a surface electrostatic potential of the gold substrate of $\psi_s = 27$ mV, with the known silica probe surface potential of $\psi_p = -37$ mV. The best fit parameters for other force data are given in Table 2. The surface charge (σ) in Table 2 is calculated from the following relationship[31]

$$\sigma = \epsilon_0 \epsilon_s \kappa (2kT/e) \sinh\left(\frac{e\psi}{2kT}\right) \qquad (2)$$

where κ is the reciprocal Debye length of the electrolyte solution, with a dielectric constant, ϵ_s, taken to be 78.49 and assumed to be independent of surface charge change, and ϵ_0 is the permittivity of free space.

The surface charge of the SDS-adsorbed gold substrate is plotted against SDS concentration in Figure 6. The surface charge is related to the amount of SDS adsorbed on the substrate, although part of the adsorbed DS^- might be associated with counterions (as are the micelles in

Table 2. Force Data Analysis Results of the Positively Charged Gold Substrate as a Function of SDS Concentration[a]

SDS conc (M)	surface potential, ψ_s (mV)	Debye length, κ^{-1} (nm)	surface charge, σ (μC/cm^2)
0	27	9.63	0.204
10^{-8}	27	9.63	0.204
10^{-7}	15	9.63	0.110
10^{-6}	3	9.63	0.022
5×10^{-6}	0	9.63	0
10^{-5}	−23	9.63	−0.172
3×10^{-5}	−33	9.63	−0.255
10^{-4}	−41	9.63	−0.328
3×10^{-4}	−51	9.63	−0.432
10^{-3}	−58	9.63	−0.513
10^{-2}	−51	7.88	−0.525

[a] Force data were obtained between a silica sphere and a positively charged gold substrate in aqueous solutions of different SDS concentrations at 25 °C and pH 5.0. The total salt concentration ($C_{SDS} + C_{NaCl}$) was maintained at 10^{-3} M for each solution except the 10^{-2} M SDS solution. $\psi_p = -37$ mV for all 10^{-3} M solutions and −34 mV for the 10^{-2} M SDS solution. For silica−gold interactions, $A_H = 1.1 \times 10^{-19}$ J.

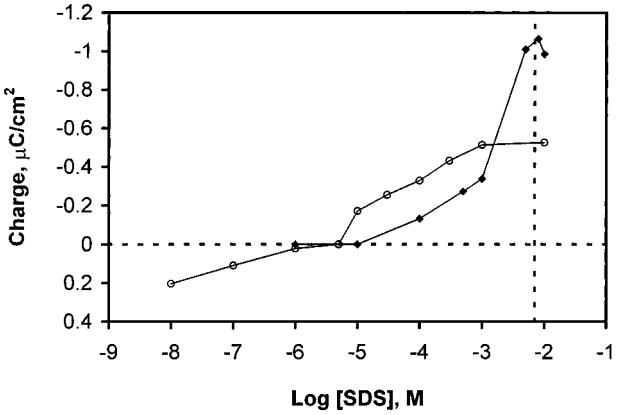

Figure 6. Plots of the surface charge vs surfactant concentration for SDS on a positively charged gold substrate (open circles) and a hydrophobic SAM-covered gold substrate (diamonds). The cmc and zero surface charge are indicated by the dotted lines.

(31) Bard, A. J.; Faulkner, L. R. *Electrochemical Methods*; J. Wiley: New York, 1980; pp 500−515.

Chart 2. Schematic of Structures of Adsorbed SDS Aggregates on a Positively Charged Gold Substrate[a]

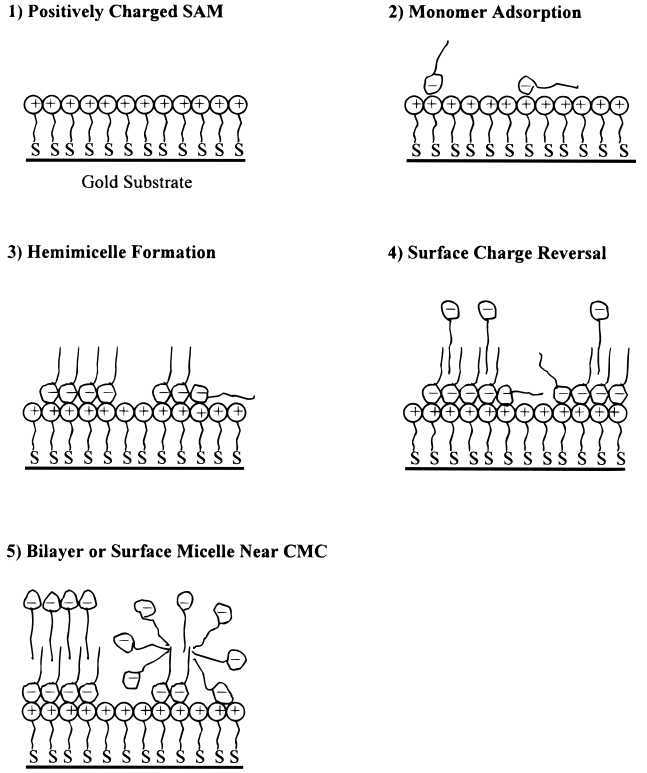

[a] At SDS concentrations near the cmc, the structures represent either bilayers or surface micelles on the substrate and should not be taken to imply coexistence of both forms.

solution). From Figure 6, certain aspects of SDS adsorption properties on a positively charged substrate are quite clear. Chart 2 illustrates the structures of adsorbed SDS aggregates on a charged surface. In very dilute SDS solutions, i.e., from 10^{-8} to 10^{-6} M, a very good linear adsorption region is observed, which is believed to be the monomer adsorption driven by electrostatic attraction between the surfactant head group and the oppositely charged surface. This linear region is followed by a plateau region where the surface charge approaches zero, probably indicating the formation of a hydrophobic hemimicelle. Above an SDS concentration of 5×10^{-6} M, another region exists where additional surfactant ions are adsorbed by hydrophobic interactions. Surface charge reversal is the significant feature of this region. Finally, a second plateau region is reached when the SDS concentration is higher than 10^{-3} M, suggesting that the adsorption is probably limited by increasing repulsion between the charged head groups or the substrate is fully covered.

Adsorption of SDS on a Hydrophobic Substrate. A self-assembled monolayer of hexadecyl mercaptan on gold was used as a model of a compact uncharged, hydrophobic substrate to mimic the adsorption properties of the hemimicelle, which was proposed to form on the charged substrate before the surface charge reversal occurred. If the hemimicelle is really a compact monolayer of surfactant exposing a hydrophobic surface to the solution, a similar adsorption behavior between the SAM and hemimicelle would be observed. The dl forces between the silica probe and the hydrophobic SAM-covered gold substrate were examined in aqueous solutions of different SDS concentrations at pH 5.0, and the force curves are given in Figure 7. Again, the total salt concentration ($C_{SDS} + C_{NaCl}$) was maintained at 10^{-3} M for each solution up to SDS concentrations of 10^{-3} M. In 10^{-3} M NaCl solution without SDS, there were no measurable long range

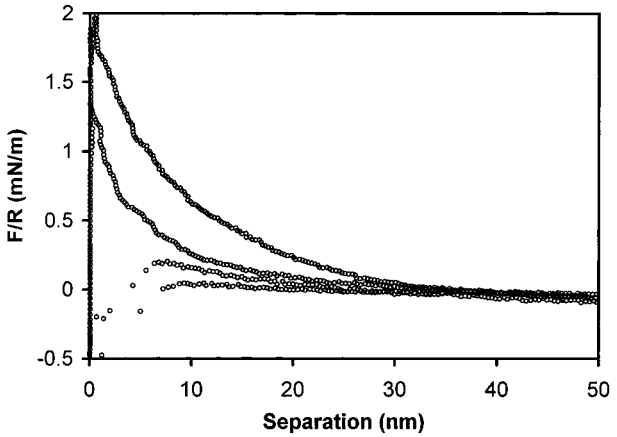

Figure 7. Force between a silica probe ($R = 8.0$ μm) and a hydrophobic SAM-covered gold substrate in aqueous solutions (pH 5.0) of (from bottom to top) 0, 10^{-4}, 10^{-3}, and 10^{-2} M SDS. The total salt concentration ($C_{SDS} + C_{NaCl}$) was maintained at 10^{-3} M for each solution except $C_{SDS} = 10^{-2}$ M.

Chart 3. Schematic of Structures of Adsorbed SDS Aggregates on a Hydrophobic SAM-Covered Gold Substrate

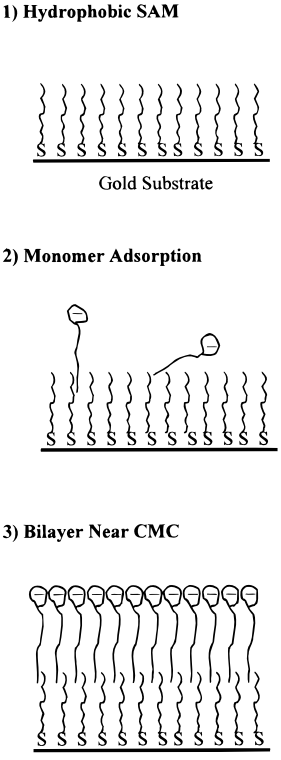

electrostatic interactions between the silica probe and the SAM-covered gold substrate, suggesting that the hydrophobic substrate was uncharged. Below SDS concentrations of 10^{-5} M, there was no significant adsorption of SDS on the substrate because no long distance repulsive or attractive electrostatic forces were detectable. A small repulsive force was measured at an SDS concentration of 10^{-4} M, indicating the beginning of the adsorption process by hydrophobic interactions, i.e., interchain penetration. This process resulted in the formation of local bilayers exposing the negative surfactant head groups to solution. With a further increase in SDS concentration, a higher negative charge built up on the substrate, thus increasing the repulsive force. These adsorption processes are schematically illustrated in Chart 3. The surface charge and potential of the SDS-adsorbed gold substrate in

Table 3. Force Data Analysis Results of the Hydrophobic SAM-Covered Gold Substrate as a Function of SDS Concentration[a]

SDS conc (M)	surface potential, ψ_s (mV)	Debye length, κ^{-1} (nm)	surface charge, σ (μC/cm^2)
0	0	0	0
10^{-6}	0	0	0
10^{-5}	0	0	0
10^{-4}	−18	9.63	−0.133
5×10^{-4}	−35	9.63	−0.273
10^{-3}	−42	9.63	−0.338
5×10^{-3}	−55	4.55	−1.010
8×10^{-3}	−87	8.81	−1.065
10^{-2}	−78	7.88	−0.984

[a] Force data were obtained between a silica sphere and a hydrophobic SAM-covered gold substrate in aqueous solutions of different SDS concentrations at 25 °C and pH 5.0. The total salt concentration ($C_{SDS} + C_{NaCl}$) was maintained at 10^{-3} M for each solution except those of $C_{SDS} > 10^{-3}$ M. $\psi_p = -37$ mV for all 10^{-3} M solutions and −30, −35, and −34 mV for 5×10^{-3}, 8×10^{-3}, and 1×10^{-2} M SDS solutions, respectively. For silica−gold interactions $A_H = 1.1 \times 10^{-19}$ J.

aqueous SDS solutions were calculated as described earlier, and the results are given in Table 3.

Figure 6 shows the surface charge vs the surfactant concentration data for SDS adsorbed on a hydrophobic SAM-covered gold substrate (diamonds), compared to those for SDS adsorbed on a positively charged gold substrate. Clearly, the SDS adsorption behavior is different for the hydrophobic SAM and the hemimicelle. First, SDS adsorption on the hydrophobic SAM occurs at higher SDS concentrations, and the amount of surface adsorption is lower than that of adsorption on the hemimicelle at SDS concentrations below 10^{-3} M. Second, the two adsorption processes reach saturation at different SDS concentrations, and the surface charge density for SDS adsorption on the hydrophobic SAM is twice that of adsorption on the hemimicelle near the cmc. From these observations, we conclude that the hemimicelle originally formed on a charged surface is not a compact and uniform monolayer of surfactants. The difference between the two adsorption processes also suggests that the surface charge reversal process proceeds without the formation of a compact monolayer of surfactants and probably occurs through local surfactant monolayers or even adsorbed monomers. Further investigation is needed to clarify if the surface charge reversal proceeds directly from adsorbed monomers or via hemimicelles.

The adsorption of SDS from aqueous solution onto a monolayer of dimethyloctadecylsiloxane bonded to silica has been previously characterized by FTIR spectroscopy[32] and produced a similar adsorption behavior to that obtained here for the hexadecyl mercaptan/Au. There was a distinct maximum in the adsorption isotherm that occurred at 7 mM. A similar maximum was also found in our adsorption curve at 8 mM. The reasons for the formation of the maximum were not clear. Nevertheless, from the adsorption isotherm, the FTIR spectral shifts, and the band widths, the adsorbed SDS was found to be organized in a dense monolayer on a hydrophobic C_{18} surface near the cmc. This dense monolayer of surfactants on a hydrophobic surface, formed by interchain penetration near the cmc, can serve as a model of the flat and uniform bilayer structure. From the surface charge density difference between SDS adsorption on a charged surface and that on a hydrophobic SAM surface near the cmc, we speculate that the formation of compact and continuous surfactant bilayer structure on a charged surface does not occur as postulated earlier.[13,33,34] Indeed, recent AFM images of ionic surfactants adsorbed onto a variety of solid surfaces strongly support this view. For example, Manne and Gaub[35] recently studied the morphology of a quaternary ammonium surfactant adsorbed on several solid surfaces above the cmc. They found that the resulting surfactant structures were full cylinders on mica, spherical micelles on amorphous silica, and half-cylinders on graphite and MoS_2 substrates. More recently, Sharma et al.[36] investigated images of CTAB molecules adsorbed on a mica surface at surfactant concentrations ranging from 10^{-5} to 10^{-2} M. At low surfactant concentration, discrete aggregates of absorbed surfactants were found on the surface. As the surfactant concentration increased, these aggregates became more organized into elongated cylindrical shapes. Wanless and Ducker[37] studied AFM images of the aggregated structure of SDS adsorbed to the graphite/solution interface in the concentration range 2.8−81 mM. Instead of uniform bilayer structures, they observed that SDS adsorbed in periodic structures with hemicylindrical geometry. In all cases, a spontaneous curvature that results from inter-head group repulsion was observed. These AFM images evidently disprove previously assumed models of flat and uniform surfactant monolayers and bilayers.

Conclusions

An AFM was used to study the ionic nature of SDS by measuring the double-layer forces between a silica probe and a silica substrate in SDS aqueous solutions. The cmc for SDS in deionized water was determined by measuring the sudden change in diffuse double-layer thickness. The adsorption of SDS was investigated by measuring the double-layer forces between a negative silica probe and either a positively charged or hydrophobic SAM-covered gold substrate over a broad range of SDS concentration. For a positively charged substrate, surface charge reversal occurred at an SDS concentration of about 1/1000 cmc. The surface electrostatic potentials of the surfactant-adsorbed substrates were calculated by solving the complete nonlinear Poisson−Boltzmann equation with the knowledge of silica probe surface potentials. The surface charge vs SDS concentration data yielded information about the surfactant adsorption mechanism. For a hydrophobic SAM substrate, the SDS adsorption behavior was found to be different from the adsorption on a hemimicelle formed on the charged substrate. These results led to the conclusion that the formation of a compact and uniform SDS hemimicelle or bilayer on a charged surface did not occur as proposed earlier.

Acknowledgment. The support of this research by grants from the Robert A. Welch Foundation and the National Science Foundation (Grant CHE-9508525) is gratefully acknowledged. The authors also thank Dr. F.-R. F. Fan for helpful discussions and Dr. Andrew C. Hillier (University of Virginia) for providing the computer program for the calculation of double-layer forces.

LA970483T

(32) Montgomery, M. E., Jr.; Wirth, M. J. *Langmuir* **1994**, *10*, 861.
(33) Bijsterbosch, B. H. *J. Colloid Interface Sci.* **1974**, *47*, 186.
(34) Iler, R. K. *The Chemistry of Silica*; J. Wiley: New York, 1979; pp 680−686.
(35) Manne, S.; Gaub, H. E. *Science* **1995**, *270*, 1480.
(36) Sharma, B. G.; Basu, S.; Sharma, M. M. *Langmuir* **1996**, *12*, 6506.
(37) Wanless, E. J.; Ducker, W. A. *J. Phys. Chem.* **1996**, *100*, 3207.